


RESEARCH

Open Access



B7H3-targeting chimeric antigen receptor modification enhances antitumor effect of V γ 9V δ 2 T cells in glioblastoma

Yi Wang^{1,2,3}, Nan Ji^{1,2,3}, Yang Zhang^{2,3}, Junsheng Chu^{2,3}, Changcun Pan^{2,3}, Peng Zhang^{2,3}, Weiwei Ma⁴, Xueguang Zhang⁵, Jianzhong Jeff Xi⁶, Mingze Chen^{2,3}, Yonghui Zhang^{4*}, Liwei Zhang^{1,2,3*} and Tao Sun^{2,3*} 

Abstract

Background Glioblastoma (GBM) is a highly aggressive primary brain tumor with a poor prognosis. This study investigates the therapeutic potential of human V γ 9V δ 2 T cells in GBM treatment. The sensitivity of different glioma specimens to V γ 9V δ 2 T cell-mediated cytotoxicity is assessed using a patient-derived tumor cell clusters (PTCs) model.

Methods The study evaluates the anti-tumor effect of V γ 9V δ 2 T cells in 26 glioma cases through the PTCs model. Protein expression of BTN2A1 and BTN3A1, along with gene expression related to lipid metabolism and glioma inflammatory response pathways, is analyzed in matched tumor tissue samples. Additionally, the study explores two strategies to re-sensitize tumors in the weak anti-tumor effect (WAT) group: utilizing a BTN3A1 agonistic antibody or employing bisphosphonates to inhibit farnesyl diphosphate synthase (FPPS). Furthermore, the study investigates the efficacy of genetically engineered V γ 9V δ 2 T cells expressing Car-B7H3 in targeting diverse GBM specimens.

Results The results demonstrate that V γ 9V δ 2 T cells display a stronger anti-tumor effect (SAT) in six glioma cases, while showing a weaker effect (WAT) in twenty cases. The SAT group exhibits elevated protein expression of BTN2A1 and BTN3A1, accompanied by differential gene expression related to lipid metabolism and glioma inflammatory response pathways. Importantly, the study reveals that the WAT group GBM can enhance V γ 9V δ 2 T cell-mediated killing sensitivity by incorporating either a BTN3A1 agonistic antibody or bisphosphonates. Both approaches support TCR-BTN mediated tumor recognition, which is distinct from the conventional MHC-peptide recognition by $\alpha\beta$ T cells. Furthermore, the study explores an alternative strategy by genetically engineering V γ 9V δ 2 T cells with Car-B7H3, and both non-engineered and Car-B7H3 V γ 9V δ 2 T cells demonstrate promising efficacy in vivo, underscoring the versatile potential of V γ 9V δ 2 T cells for GBM treatment.

Conclusions V γ 9V δ 2 T cells demonstrate a robust anti-tumor effect in some glioma cases, while weaker in others. Elevated BTN2A1 and BTN3A1 expression correlates with improved response. WAT group tumors can be sensitized using a BTN3A1 agonistic antibody or bisphosphonates. Genetically engineered V γ 9V δ 2 T cells, i.e., Car-B7H3, show promising efficacy. These results together highlight the versatility of V γ 9V δ 2 T cells for GBM treatment.

*Correspondence:

Yonghui Zhang

zhangyonghui@tsinghua.edu.cn

Liwei Zhang

zhanglw@bjtth.org

Tao Sun

suntao@bjtth.org

Full list of author information is available at the end of the article



© The Author(s) 2023. **Open Access** This article is licensed under a Creative Commons Attribution 4.0 International License, which permits use, sharing, adaptation, distribution and reproduction in any medium or format, as long as you give appropriate credit to the original author(s) and the source, provide a link to the Creative Commons licence, and indicate if changes were made. The images or other third party material in this article are included in the article's Creative Commons licence, unless indicated otherwise in a credit line to the material. If material is not included in the article's Creative Commons licence and your intended use is not permitted by statutory regulation or exceeds the permitted use, you will need to obtain permission directly from the copyright holder. To view a copy of this licence, visit <http://creativecommons.org/licenses/by/4.0/>. The Creative Commons Public Domain Dedication waiver (<http://creativecommons.org/publicdomain/zero/1.0/>) applies to the data made available in this article, unless otherwise stated in a credit line to the data.

Keywords V γ 9V δ 2 T cells, Glioblastoma, B7-H3, BTN2A1, BTN3A1

Background

Glioblastoma (GBM) is the most common primary malignant brain tumor, accounting for 48.6% of all primary brain malignancies. It is classified as a grade IV glioma according to the World Health Organization (WHO) classification [1, 2]. Despite standard-of-care treatments such as surgical resection and radiotherapy, the median survival of GBM patients is only 15–20 months [3], and the prognosis remains poor with a 5 year survival rate of only 5.4% [4]. Thus, it is crucial to develop effective therapeutic strategies to enhance the prognosis of GBM patients.

Immunotherapy has shown promising results in the treatment of malignant tumors [5, 6]. However, the effectiveness of immunotherapy in treating GBM remains uncertain [7]. One of the most recent immunotherapy modalities for GBM is the adoptive transfer of $\gamma\delta$ T lymphocytes expressing a T cell receptor (TCR) composed of γ and δ chains [8, 9]. In healthy peripheral blood, $\gamma\delta$ T cells expressing the V γ 9V δ 2 chain account for 5–10% of CD3⁺ cells, representing the main subset of peripheral $\gamma\delta$ T cells [10]. Zoledronic acid (ZOL) can inhibit the farnesyl diphosphate synthase in the mevalonate pathway, resulting in the accumulation of the upstream molecules isopentenyl pyrophosphate (IPP) and dimethylallyl pyrophosphate (DMAPP) [11]. V γ 9V δ 2 T cells detect changes in the IPP level of target cells through receptors such as TCR, thereby activating themselves and killing tumor cells. A breakthrough in understanding the possible mechanisms of IPP-mediated V γ 9V δ 2 T cells activation was the discovery that butyrophilin subfamily 2 member A1 (BTN2A1) and BTN3A1 are essential for V γ 9V δ 2 T cells activation [12, 13]. Activation of V γ 9V δ 2 T-cell receptor clonotypes can be induced by the BTN3A1-specific antibody 20.1 [14]. Like natural killer cells, V γ 9V δ 2 T cells express NKG2D receptors that can recognize MHC class I-related chain proteins A and B (MICA/B) on GBM cells [15–17]. Thus, V γ 9V δ 2 T cell immunotherapy is a promising therapeutic strategy for GBM treatment [18].

Despite significant progress in immunotherapy, chimeric antigen receptor (CAR)-T cell therapy based on $\alpha\beta$ T cells has yet to achieve a breakthrough in treating solid tumors due to several limitations, such as T cell-associated toxicities, limited efficacy against solid tumors, antigen escape, poor trafficking and tumor infiltration, and the immunosuppressive microenvironment within the tumor [19, 20]. However, studies have shown that $\gamma\delta$ T cells may serve as an alternative

source of CAR-T cells [21, 22]. B7-H3 of the B7 family is highly expressed in over 70% of GBM specimens [23], and B7-H3-targeting immunotherapies are currently under clinical investigation in children and adults with refractory extracranial solid tumors and brain tumors (NCT02982941, NCT01391143, and NCT04185038) [24–26]. Therefore, we hypothesized that $\gamma\delta$ T cells targeting B7-H3 could effectively suppress GBM development.

This study investigated the safety and antitumor effects of V γ 9V δ 2 T cells and Car-B7H3- $\gamma\delta$ T cells derived from healthy human peripheral blood mononuclear cells (PBMCs), and tested them against GBM cell lines, primary GBM cells, patient-derived tumor cell clusters (PTCs), and a mouse GBM model. We also conducted a preliminary investigation into the mechanism underlying the different responses of PTCs to V γ 9V δ 2 T cell therapy. Several methods were explored to enhance the anti-glioma ability of V γ 9V δ 2 T cells. The findings suggest that Car-B7H3- $\gamma\delta$ T cell immunotherapy has significant potential as a well-tolerated therapeutic approach for treating GBM.

Methods

Preparation of V γ 9V δ 2 T cells and car-B7H3- $\gamma\delta$ T cells

PBMCs were obtained from healthy subjects aged 18–50 years with a platelet count of $\geq 100 \times 10^9/L$ and activated partial thromboplastin time and prothrombin time within the normal range at Beijing Tiantan Hospital, China. Exclusion criteria: hematological diseases, steroid use within one month, and all malignancies. All participants provided signed informed consent. V γ 9V δ 2 T cells were expanded using a previously described method [27]. Briefly, the PBMCs was isolated by Ficoll gradient (17544602, Cytiva, USA) from leukapheresis from healthy donors. GMP-compliant serum-free medium containing 200 U/mL IL2 and 2 mM L-glutamine (Gibco—Thermo Fisher Scientific, Waltham, MA, USA) was used to promote cell expansion. Zoledronic acid (5 μ M, Sigma-Aldrich, St. Louise, MO, USA) was added to the medium on day 0 of cultivation and the cell concentration was 2×10^6 cells/ml. The cells were incubated at 37 °C, 5% CO₂. The cell density was modified to 1×10^6 cells/ml during the culture process every 2–3 days. On day 10, the number of V γ 9V δ 2 T cells was detected. The purity of V γ 9V δ 2 T cells was determined by flow cytometry. The cells were stained with anti-human TCR V δ 2-PerCP antibodies (BioLegend, clone: B6).

To generate Car-B7H3- $\gamma\delta$ T cells, we constructed a CAR from HIV-1-derived lentivirus vectors containing a mouse Ig Kappa leader sequence, CD8 α hinge and transmembrane domains, and CD28, 4-1BB, and CD3 ζ endo domains (FVPVFLPAKPTTTPAPRPPT-PAPTIASQPLSLRPEACRPAAGGAVHTRGLDFACDI-YIWAPLAGTCGVLLLSLVITLYCNHRNRSKRSRLHSDYMNMTPRRPGPTRKHYQPYAPPRDFAAYRSRFSVVKRGRKLLLYIFKQPFMRPVQTTQEEDGCSCRFPEEEEGGCELRVKFSRSADAPAYQQGQNQLYNELNLGRREEYDVLKRRGRDPEMGGKPRRKNPQEGLYNELQKDKMAEAYSEIGMKGERRRGKGDGLYQGLSTATKDTYDALHMQUALPPR). The configuration of the intracellular domain in the third generation of CAR CD28 can enhance the function of CAR-T cells. Additionally, the presence of the 4-1BB intracellular domain structure can contribute to the persistence of CAR-T cells [28, 29]. The scFv of the anti-B7-H3 antibody, consisting of heavy and light chains fused with a (GGGS)₃ linker, was inserted between the mouse Ig Kappa signal sequence and the CD8 α hinge domain, resulting in the B7-H3-CD28/4-1BB/CD3 ζ -CAR construct. A truncated version of the epidermal growth factor receptor (EGFR) was co-expressed with a P2A cleavage peptide on the C terminal of the CAR construct. The CAR expression was monitored by measuring EGFR expression. On day 10 after expansion, Car-B7H3- $\gamma\delta$ T cells were obtained by transfecting V γ 9V δ 2 T cells with B7-H3-CD28/4-1BB/CD3 ζ -CAR, and the purity was characterized using flow cytometry.

Human GBM tumor cell lines and cell culture

U-87MG, TJ905, and HTB15 cell lines (ATCC, Manassas, VA, USA) were maintained in DMEM (Gibco) supplemented with L-glutamine (Corning, Corning, NY, USA), 10% FBS, and 1% penicillin–streptomycin (Gibco) in a humidified atmosphere with 5% CO₂ at 37 °C. All cell lines were stably transfected with lentiviral luciferase vectors to generate U-87MG-Luc, TJ905-Luc, and HTB15-Luc cells.

Human glioma tumor specimens, primary cells, and PTCs

This study was approved by the Ethics Committee of Beijing Tiantan Hospital (KY2014-021–02). Human glioma tumor specimens (n=26) were obtained from patients enrolled in the Neurosurgery Clinical Information and Biobank Project of the Department of Brain Oncology, Beijing Tiantan Hospital, during tumor resection surgery. The patients were aged 18–72 years and were diagnosed with glioma based on histopathological examination. The tumor specimens were divided into three parts: one part was used to generate PTCs, an organoid tumor model for preclinical drug testing [30]. PTCs were cultured in RPMI

medium (HyClone, Logan, UT, USA) and used for drug testing within 2 weeks after obtaining the tumor samples, as previously described [25, 30]. Another part was used to generate primary cells, which were cultured in 1% matrigel (356,243, BD, 4–12 h at 37 °C)-coated plates with serum-free DMEM (C11995500BT, Invitrogen), B27 (1:50), N2 (1:100), insulin (20 μ g/mL), bFGF (20 ng/mL), EGF (20 ng/mL), PDGF-AB (20 ng/mL) (PeproTech). All primary cells were stably transfected with lentiviral luciferase vectors. The last part of the tumor specimens was used for RNA sequencing (RNA-Seq). The clinical information of the patients was summarized in Additional file 1: Table S1.

Flow cytometry

The human GBM cell surfaces were stained with 10 μ g/mL APC-labeled anti-human MICA/B mAb (#320908; Biolegend, San Diego, CA, USA), FITC-labeled anti-human BTN2A1 pAb (#orb499606; Biorbyt, UK), FITC-labeled anti-human BTN3A1 mAb (#14-2779-82; Invitrogen, Waltham, MA, USA), APC-labeled anti-human B7H3 (#351005; Biolegend), APC-labeled anti-human EGFR (#352906; Biolegend), or corresponding isotype control. The stained cells were analyzed using a FACS Calibur flow cytometer (Becton Dickinson, Franklin Lakes, NJ, USA).

Coculture of T cells with GBM cells or PTCs

To assess the antitumor effects of V γ 9V δ 2 T cells or Car-B7H3- $\gamma\delta$ T cells, we incubated them with GBM cells or PTCs. Purified V γ 9V δ 2 T cells or Car-B7H3- $\gamma\delta$ T cells were centrifuged for 5 min at 300 g and resuspended in DMEM medium. T cells were then cocultured with target cells (U-87MG-Luc, TJ905-Luc, and HTB15-Luc cell lines) at different effective target (E:T) ratios of 0:1, 0.2:1, 0.5:1, 1:1, or 3:1 in the presence of interleukin 2 (IL-2) in a 96-well plate for 18–20 h at 37 °C. The luciferase activity was measured using a Bright-Lite luciferase detection system (#DD1204-01; Vazyme, Nanjing, China). The supernatant was collected to measure IFN- γ (#abs510007; Absin) and TNF- α (#abs510006; ABSIN) levels by ELISA.

To evaluate the antitumor effect of V γ 9V δ 2 T cells on PTCs (n=26), V γ 9V δ 2 T cells were cocultured with each sample at a ratio of 3:1. The antitumor effect was assessed by measuring the diameter changes of PTCs at 8 h after incubation using a confocal high-content imaging microscope (Opera Phenix). The antitumor effect was calculated as (the diameter of PTCs after coculture/the diameter of PTCs before coculture) \times 100%. Patients were categorized into two types according to the antitumor effect: those with an antitumor effect \geq 50% were defined as having a stronger antitumor effect (SAT), while those

with an antitumor effect <50% were defined as having a weaker antitumor effect (WAT).

ZOL or BTN3A1 agonistic monoclonal antibody stimulation

To investigate whether the addition of ZOL or BTN3A1 agonistic monoclonal antibody could enhance the killing effect of V γ 9V δ 2 T cells against WAT primary glioma cells (TT-LS, TT-YZJ, TT-ZLH, TT-XJ, TT-SX, and TT-HCL), V γ 9V δ 2 T cells were co-cultured with insensitive primary glioma cells at a 1:1 ratio for 18 to 20 h. The co-cultures were supplemented with ZOL (at a working concentration of 5 μ M, Sigma), activating BTN3A1 agonistic monoclonal antibody (eBioBT3.1 (20.1, BT3.1), eBio-science™), or a control. The luciferase activity was then measured.

U87-B7H3-KO (B7H3 knocked out) cells stably transfected with lentiviral luciferase vectors were kindly provided by Dr. Xueguang Zhang from Soochow University. To assess whether Car-B7H3- γ δ T cells retained their function as V γ 9V δ 2 T cells, Car-B7H3- γ δ T and V γ 9V δ 2 T cells were co-cultured with U87-B7H3-KO cells in 1:1 ratio for 18 to 20 h in the presence or absence of ZOL (5 μ M working concentration, Sigma). The luciferase activity was measured.

Orthotopic xenograft glioma model

Immunodeficient NSG mice (NOD.Cg-Prkdcscid Il2rgtm1Wjl/Sz), 6–8 weeks old, weighing 20–25 g) were obtained from Sperf Biotech, Beijing, China, and housed under specific-pathogen-free conditions at 22 \pm 1 $^{\circ}$ C, 50 \pm 1% humidity, with a 12/12 h light/dark cycle and free access to water and a Chow diet. All animal procedures were conducted following the guidelines of the Beijing Neurosurgical Institute Laboratory Animal Welfare and Ethics Committee (BNI Approval Number: 202202002) and in accordance with the AAALAC and IACUC Guidelines. The study was approved by the Beijing Regional Ethics Committee.

Each mouse received an intracranial injection of 5 μ L phosphate-buffered saline (PBS) containing 10⁵ U-87MG-Luc cells at a rate of 1 μ L/min using a stereotactic tumor establishment device. The coordinates for the injection were 2 mm to the right from the bregma and 3.5 mm depth. Six to nine days after injection, mice were intraperitoneally injected with 150 ng/g D-luciferin (#122,796; PerkinElmer, Waltham, MA, USA). Tumor formation was observed and imaged using an IVIS system (Caliper Life Sciences, Mountain View, CA, USA) after 10 min of injection. The IVIS data was analyzed using the Living Image software (Caliper Life Sciences). Tumor formation was also confirmed by MRI examination.

The tumor-bearing mice were randomly divided into three groups: V γ 9V δ 2 T cell group, Car-B7H3- γ δ T cell

group, and control group (n=5/group). Each mouse received an intracranial injection of 5 \times 10⁶ V γ 9V δ 2 T cells or Car-B7H3- γ δ T cells or PBS into the lateral ventricle (0.5 mm behind bregma, 1 mm left, 3 mm depth). The mice were then intraperitoneally injected with 100 μ L of IL-2 (5000 IU) twice, at 3 day intervals. The control group was injected with PBS. The mice were weighted twice a week to monitor body weight changes. Bioluminescence intensities of the tumors were measured once a week.

Cytokine multiplex assay

Cytokine multiplex assay was conducted to evaluate the safety of T cell therapy in mice. Blood samples were collected from the retrobulbar sinus, and serum was obtained by centrifuging the blood samples at 5000 g for 5 min and stored at – 80 $^{\circ}$ C until use. Serum cytokine levels were measured using a cytokine array kit (#QAH-INF-3–2, QAH-GF-1–2; RayBiotech, Peachtree Corners, GA, USA) following the manufacturer's instructions. The fluorescence intensities were measured using an Axon scanner 4000B and GenePix software. The results were analyzed using a RayBio analysis tool. For each cytokine, the mean fluorescence intensity was calculated, and the z-score was generated. A heatmap of the z-scores ranging from – 3 to 3 was generated using ggplot2 v3.2.1.

Immunohistochemistry (IHC) and multiplex immunofluorescence staining (MIS)

Human glioma tissue samples were fixed with 4% paraformaldehyde, embedded in paraffin, and cut into 5 μ m-thick sections. The tissue sections were deparaffinized, rehydrated, and underwent heat-induced epitope repair retrieval. Then, the sections were incubated with anti-BTN2A1 (1:200; #orb499606; Biorbyt) or anti-BTN3A1 (1:400; #CAB10288; Genie) antibodies at 4 $^{\circ}$ C, followed by incubation with a secondary antibody (1:1000; #ZB-2301; ZSGB-BIO, Beijing, China) for 1 h. DAB peroxidase substrate solution staining, hematoxylin blue staining, and differentiation reverse blue staining were performed. The slides were scanned using NanoZoomer 2.0 HT (Hamamatsu Photonics KK, Hamamatsu, Japan). The positive rate was calculated as (the number of positive cells/the number of total cells) \times 100%. An IHC score was calculated as the positive rate \times staining intensity. An IHC score > 10 was considered positive.

MIS was conducted in glioma tissue samples from mice to evaluate the infiltration of V γ 9V δ 2 T cells into tumors using an OPAL™ 7-color Manual IHC kit (#NEL811001 KT; Akoya Bioscience, Marlborough, MA, USA) following the manufacturer's protocol. The detailed

experimental procedures and conditions are summarized in Additional file 1: Table S2.

RNA-Seq

RNA-Seq was performed using glioma tissue samples from patients. DESeq2 (version 1.32.0) was used to identify differentially expressed genes (DEGs) with $|\text{fold change}| > 2$ and adjusted P -value < 0.05 . Gene set enrichment analysis (GSEA) was performed on hallmark gene sets from the Molecular Signatures Database (MSigDB, v7.2) to analyze the enrichment of biological pathways.

Statistical analysis

Statistical analysis was performed using the SPSS software (version 24.0; SPSS, Chicago, IL, USA). Categorical data were compared using chi-squared test or Fisher's exact test. Continuous data were compared using Student's t -test or non-parametric test. Kaplan–Meier analysis was used to estimate overall survival. A comparison between two groups was conducted using the Mann–Whitney U -test. A two-tailed P -value < 0.05 was considered significant. The plots were generated using Prism 6 (GraphPad Software, San Diego, CA, USA) and the R2 package.

Results

V γ 9V δ 2 T cells inhibit GBM cell proliferation in vitro

To expand V γ 9V δ 2 T cells from healthy human PBMCs more rapidly and efficiently, we applied serum-free media containing amino bisphosphonates as previously described [27]. We obtained V γ 9V δ 2 T cells with a purity of around 90% within 10 days (Fig. 1A). To evaluate the cytotoxicity of V γ 9V δ 2 T cells, we co-cultured V γ 9V δ 2 T cells with GBM-Luc cells at different E:T ratios in the presence of IL-2. As shown in Fig. 1B, V γ 9V δ 2 T cells inhibited GBM cell proliferation in a dose-dependent manner, as evidenced by decreased luciferase activity of the cocultures ($P < 0.05$). The most prominent antitumoral activity of V γ 9V δ 2 T cells was observed in U87-MG-Luc cells. Additionally, V γ 9V δ 2 T cells produced IFN- γ and TNF- α when cocultured with GBM cell lines

(all $P < 0.0001$) (Fig. 1C, D). These results suggest that V γ 9V δ 2 T cells inhibit GBM cell proliferation possibly by producing IFN- γ and TNF- α .

V γ 9V δ 2 T cell therapy suppresses GBM growth and improves prognosis in mice

We established a GBM mouse model by injecting U87-MG-Luc cells into the frontal cortex of mice, followed by V γ 9V δ 2 T cell therapy (Fig. 1E). The cell line-derived xenograft model was confirmed by MRI imaging (Fig. 1F), bioluminescence analysis (Fig. 1G), and hematoxylin and eosin (H and E) staining (Additional file 1: Figure S1). The tumor-bearing mice were randomly treated with V γ 9V δ 2 T cells or PBS, infused back into the lateral cerebral ventricle. We found that compared with PBS vehicle, V γ 9V δ 2 T cell therapy dramatically suppressed GBM tumor growth in mice (Fig. 1G, H) and improves survival (42 days vs. 23 days, $P < 0.0001$) (Fig. 1I) without changing the body weights of mice. These data suggest that V γ 9V δ 2 T cells can effectively suppress GBM growth and improve prognosis in vivo.

The anti-tumor activities of V γ 9V δ 2 T cell therapy vary depending on the PTC being treated

PTC is an emerging preclinical drug-testing model [30]. To evaluate the clinical significance of V γ 9V δ 2 T cell therapy, we co-cultured V γ 9V δ 2 T cells with different PTCs (Additional file 1: Table S1) at a 3:1 ratio in the presence of IL-2 for 8 h. We observed significant differences in the responses to V γ 9V δ 2 T cells among the PTCs, with SAT responses in six PTCs (1 grade II glioma, 1 grade III glioma, and 4 GBM) and WAT responses in twenty PTCs (6 grade II glioma, 4 grade III glioma, and 10 GBM) (Fig. 2A). No significant correlation was observed between the antitumor effect of V γ 9V δ 2 T cells and tumor grade ($P > 0.05$) (Additional file 1: Table S3). This finding suggests that V γ 9V δ 2 T cell therapy might be effective for some GBM patients, but additional factors beyond tumor grade may affect the therapy's effectiveness.

(See figure on next page.)

Fig. 1 Preparation of V γ 9V δ 2 T cells and their inhibition of glioblastoma in vitro and in vivo. **A** A total of 2×10^6 peripheral blood mononuclear cells (PBMCs) were obtained from healthy human donors and expanded using GMP-compliant serum-free medium containing bisphosphonate compounds and factors. Flow cytometry was performed to determine the purity of V γ 9V δ 2 T cells on day 10 after cultivation ($n = 4$). **B** V γ 9V δ 2 T cells were incubated with U-87MG-Luc, TJ905-Luc, or HTB15-Luc cells at different effective target (E:T) ratios of 0:1, 0.5:1, 1:1, or 3:1 in the presence of IL-2. The cell viability of GBM cells was determined by measuring luciferase activity after 18–20 h. Data are expressed as the mean \pm standard deviation (SD). * $P < 0.05$, ** $P < 0.01$, *** $P < 0.001$. **C, D** ELISA was performed to measure IFN- γ and TNF- α levels in the culture medium. Data are expressed as the mean \pm SD. * $P < 0.05$, *** $P < 0.001$, **** $P < 0.0001$; $n = 3$. **E** An NSG mouse GBM model was established by intracerebroventricular injection of U87-MG-Luc cells. Mice were treated with V γ 9V δ 2 T cells or PBS ($n = 8$). A workflow diagram is shown. **F** MRI imaging was performed to visualize the tumor (red arrow). **G** Bioluminescence images of the mouse brain were taken on day 8, 12, and 19 after injection. **H** Bioluminescence intensity was measured to examine tumor growth. Data are expressed as the mean \pm SD. **** $P < 0.0001$. **I** Kaplan–Meier survival analysis was performed

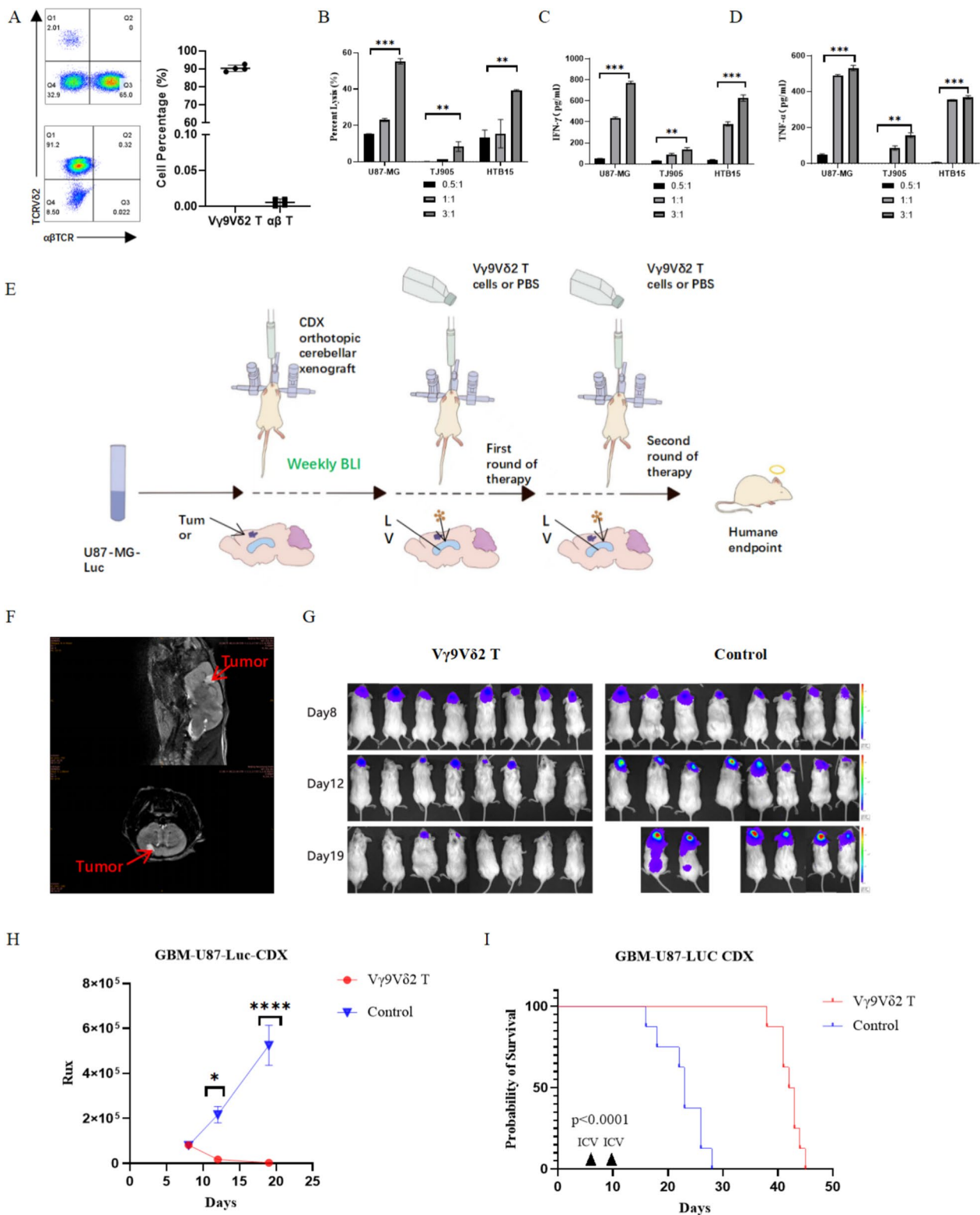


Fig. 1 (See legend on previous page.)

BTN2A1 and BTN3A1 expression correlates with the antitumor activity of V γ 9V δ 2 T cells

Since V γ 9V δ 2 T cells can recognize tumor cells expressing BTN2A1 and BTN3A1 [12, 31, 32], we compared the expression of these two molecules in different GBM cell lines by flow cytometry and matched tumor samples of PTCs using IHC staining. Our results showed that BTN2A1 and BTN3A1 were highly expressed in U87-MG cell line (Additional file 1: Figure S2A) and the SAT group (Fig. 2B, D), compared to the WAT group (Fig. 2C, E). Furthermore, the BTN2A1 and BTN3A1 IHC scores were significantly higher in the SAT group than in the WAT group (Fig. 2F, G). Specifically, all samples in the SAT group were double-positive for BTN2A1 and BTN3A1, while only a small fraction of the WAT group samples were BTN2A1-positive (15%), BTN3A1-positive (25%), or double-positive (15%) (Table 1). No BTN2A1 or BTN3A1 expression was detected in tumor-adjacent tissue or normal brain tissue. In addition, no significant correlation was observed between BTN2A1/BTN3A1 protein expression and WHO grade ($P > 0.05$) (Table 2). These results suggest that V γ 9V δ 2 T cells may inhibit GBM growth by targeting BTN2A1 and BTN3A1 on GBM tumor cells.

To explore the molecular mechanisms involved in the antitumor activity of V γ 9V δ 2 T cells in GBM, we performed RNA-seq to identify DEGs between SAT and WAT tissue samples and used GSEA to analyze the enriched pathways. Our results revealed that V γ 9V δ 2 T cell response was mainly related to fatty acid metabolism, primary bile acid biosynthesis, nicotinate and nicotinamide metabolism, peroxisome, ABC transporters, tryptophan metabolism, arachidonic acid metabolism, glycerolipid metabolism, proximal tubule bicarbonate reclamation, TGF beta signaling pathway, and PPAR signaling pathway (Fig. 2H–J). These data suggest that lipid metabolism and glioma inflammatory response may play important roles in the antitumor effect of V γ 9V δ 2 T cells on GBM.

ZOL or BTN3A1 agonistic antibody enhances the antitumor activity of V γ 9V δ 2 T cells in glioma

To investigate the potential of enhancing the antitumor activity of V γ 9V δ 2 T cells in insensitive glioma, we

co-cultured V γ 9V δ 2 T cells with WAT primary glioma cells (TT-LS-luc, TT-YZJ-luc, TT-ZLH-luc, TT-XJ-luc, TT-SX-luc, and TT-HCL-luc) at E:T ratios of 1:1 in the presence or absence of ZOL or BTN3A1 agonistic antibody. Our results showed that the killing of V γ 9V δ 2 T cells against primary glioma cells was significantly enhanced after ZOL (Fig. 3A) or BTN3A1 agonistic antibody stimulation (Fig. 3B). These findings suggest that ZOL and BTN3A1 agonistic antibody can stimulate glioma cells to enhance their sensitivity to V γ 9V δ 2 T cells. However, since the safety of these two drugs has not been confirmed for intracerebroventricular injection, they cannot be used in clinical treatment of glioma at present.

Car-B7H3- γ δ T cells maintain a functional endogenous TCR

To address this issue, we transfected V γ 9V δ 2 T cells with plasmids (Fig. 3C) containing the scFv of the anti-B7-H3 antibody and obtained Car-B7H3- γ δ T cells with a purity of around 69.5% (Additional file 1: Figure S2B). Because the V γ 9V δ 2 TCR is activated by accumulation of phosphoantigens induced by bisphosphonates such as ZOL, we tested whether Car-B7H3- γ δ T cells maintained the functionality of their endogenous TCR [33]. When V γ 9V δ 2 T cells or Car-B7H3- γ δ T cells were co-cultured with U87-B7H3-KO at an E:T ratio of 1:1 and stimulated with ZOL, both types of T cells showed enhanced cytotoxic effects (Fig. 3D). These results suggest that Car-B7H3- γ δ T cells can still be stimulated by ZOL to enhance their antitumor effect, similar to V γ 9V δ 2 T cells.

Car-B7H3- γ δ T cells exhibit stronger anti-glioma activity than parental V γ 9V δ 2 T cells in vitro

To evaluate the potential of Car-B7H3- γ δ T lymphocytes in clinical settings, we examined the expression of B7-H3 in six primary cell lines generated from the WAT group. All six cell lines were IDH wild type, among which three had unmethylated MGMT promoters (TT-LS, TT-YZJ, and TT-ZLH) and three had methylated MGMT promoters (TT-XJ, TT-SX, and TT-HCL). Flow cytometry results showed that B7-H3 was highly expressed in all six primary cell lines (positive rate > 90%) (Fig. 3E). Similarly, flow analysis revealed that B7-H3 was highly expressed

(See figure on next page.)

Fig. 2 V γ 9V δ 2 T cell therapy exhibited different anti-tumor activities on patient-derived tumor cell clusters (PTCs) **A** GBM patients (n = 26) were categorized into two groups according to the antitumor effects of V γ 9V δ 2 T cells on matched PTCs by co-culture killing assay: stronger anti-tumor effect (SAT; n = 6) and weaker anti-tumor effect (WAT; n = 20) groups **B–E** Immunohistochemical (IHC) staining was performed to detect BTN2A1 **B, C** and BTN3A1 **D, E** expression in tumor tissue samples from patients in the SAT **B, D** and WAT **C, E** groups. **F, G** IHC scores were calculated. **H** RNA sequencing was performed on glioma tissue samples from patients. A heatmap of differentially expressed genes (DEGs; |fold change| > 2 and adjusted P -value < 0.05) in patients with SAT versus those with WAT is shown. **I** A volcano plot of the DEGs is displayed. **J** KEGG analysis of the DEGs was conducted. The top 14 enriched pathways are shown

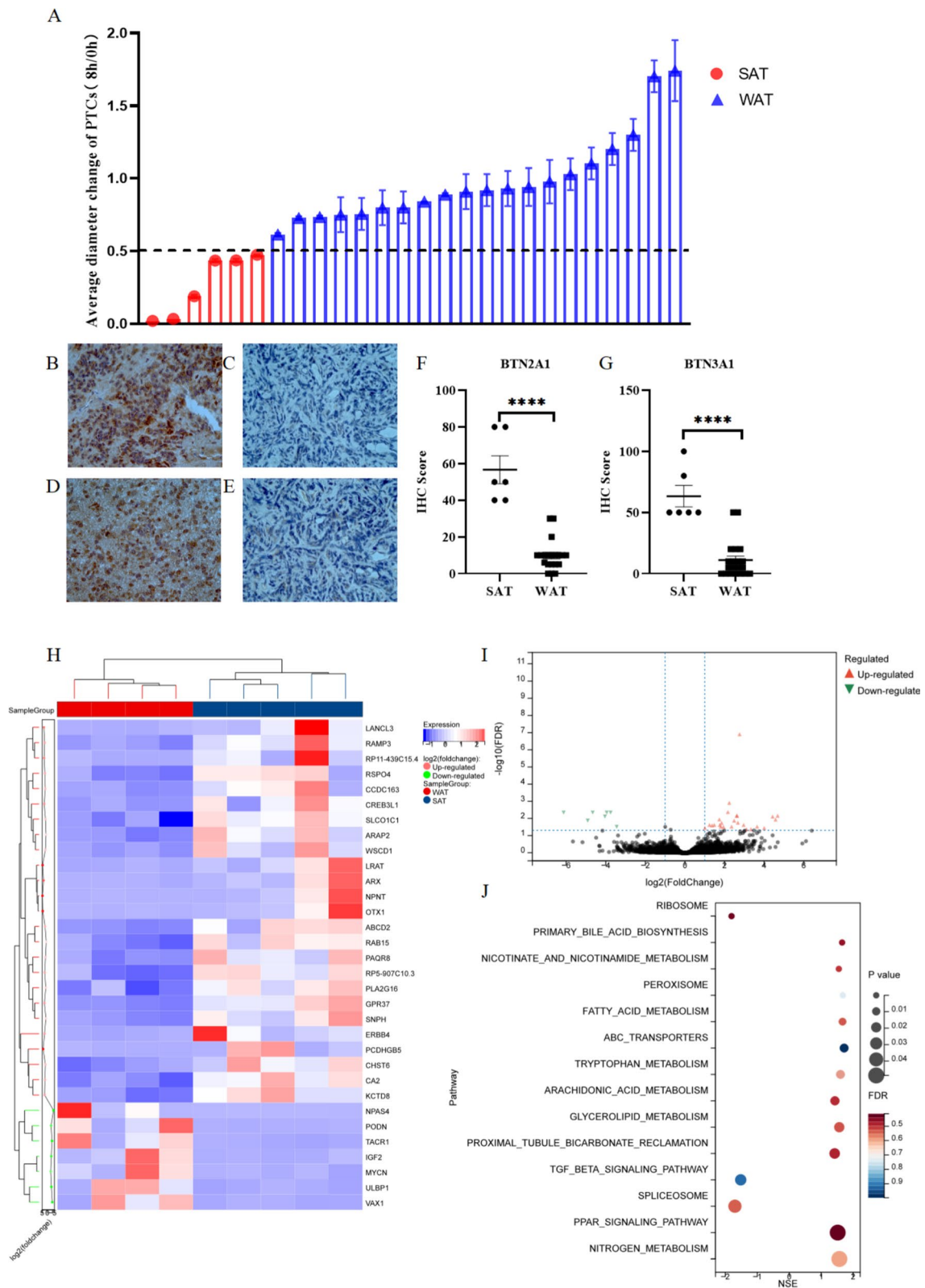


Fig. 2 (See legend on previous page.)

Table 1 Immunohistochemistry analysis of BTN2A1 and BTN3A1 expression in tumor tissue samples of glioma patients with different responses to V9V62 T therapy

Antitumor effect on PTCs	Total patients (n)	BTN2A1 Expression		BTN3A1 Expression		BTN2A1 + BTN3A1 expression		P value*
		Positive (n)	Negative (n)	Positive (n)	Negative (n)	Positive (n)	Negative (n)	
SAT	6	6	0	6	0	6	0	100
WAT	20	3	17	5	15	3	17	15
								0.00012

SAT stronger anti-tumor effect, WAT weaker anti-tumor effect

* Chi-squared tests

Table 2 Immunohistochemistry analysis of BTN2A1 and BTN3A1 expression in tumor tissue samples from patients with different grades of glioma

WHO grade	Total Patients (n)	BTN2A1 Expression		Positive Rate (%)	BTN3A1 Expression		Positive Rate (%)	P Value
		Positive (n)	Negative (n)		Positive (n)	Negative (n)		
II	7	2	5	29	2	5	29	
III	5	1	4	20	2	3	40	> 0.05
IV	14	6	8	43	7	7	50	

on the surface of U-87MG, TJ905, and HTB15 cells (Additional file 1: Figure S2C).

We co-cultured V γ 9V δ 2 T and Car-B7H3- γ δ T cells with the six primary cell lines at different E:T ratios in the presence of IL-2. As shown in Fig. 3E, at the same E:T ratio (1:1), Car-B7H3- γ δ T cells significantly inhibited the proliferation of all six primary cell lines, while V γ 9V δ 2 T cells were insensitive (all $P < 0.05$). Additionally, Car-B7H3- γ δ T cells produced more IFN- γ and TNF- α when cocultured with primary WAT cells (all $P < 0.05$) (Fig. 3G, H). Similarly, at the same E:T ratio, Car-B7H3- γ δ T cells exhibited a more potent inhibitory effect on GBM cell line proliferation than V γ 9V δ 2 T cells ($P < 0.05$) (Additional file 1: Figure S2D). Moreover, Car-B7H3- γ δ T cells secreted more cytokines than V γ 9V δ 2 T cells ($P < 0.05$) (Additional file 1: Figure S2E). These data suggest that Car-B7H3- γ δ T cells exhibit stronger and wider anti-glioma activity than parental V γ 9V δ 2 T cells in vitro.

Car-B7H3- γ δ T cells demonstrate stronger inhibition of GBM growth in mice compared to V γ 9V δ 2 T Cells

To evaluate the antitumor effects of V γ 9V δ 2 T and Car-B7H3- γ δ T cells in vivo, we established a GBM PDX mouse model by injecting U87-MG-Luc cells into the frontal cortex. In vivo, bioluminescence was performed weekly to monitor tumor size, and then V γ 9V δ 2 T or Car-B7H3- γ δ T cells or PBS were infused into the lateral cerebral ventricle once a week for two weeks. Bioluminescence analysis showed that tumors were formed in the mouse brain on day 7 after tumor cell injection

(Fig. 4A). Both V γ 9V δ 2 T and Car-B7H3- γ δ T cell treatments significantly suppressed GBM tumor growth in mice compared to the vehicle control (Fig. 4A). Notably, Car-B7H3- γ δ T cells demonstrated a stronger inhibition of mouse brain tumor growth than V γ 9V δ 2 T cells ($P < 0.0001$) (Fig. 4B). Moreover, the survival of both the Car-B7H3- γ δ T and V γ 9V δ 2 T groups was significantly longer than that of the control group (44 and 38 days vs. 28 days; both $P < 0.0001$), and the survival of the Car-B7H3- γ δ T group was longer than that of the V γ 9V δ 2 T group (44 days vs. 38 days, $P < 0.0001$) (Fig. 4C). These data suggest that Car-B7H3- γ δ T cells demonstrate stronger inhibition of GBM growth and improve prognosis in vivo compared to V γ 9V δ 2 T cells.

V γ 9V δ 2 T and Car-B7H3- γ δ T cells infiltrate into GBM tumors in mice after intracranial injection

We injected V γ 9V δ 2T or Car-B7H3- γ δ T cells into the lateral ventricle of orthotopically implanted mouse models. Opal multi-dimensional fluorescence staining was performed on tumor tissues harvested on day 1, day 7, and day 14 after infusion. TCR δ 2 labeled V γ 9V δ 2 T cells, B7-H3 labeled Car-B7H3- γ δ T cells, and Granzyme B was used to label activated T cells (killing activity) (Fig. 5A, B). On day 1, both V γ 9V δ 2 T and Car-B7H3- γ δ T cells infiltrated the brain stem tumor of mice, with a small number of cells becoming activated and beginning to play a role in killing. Furthermore, the infiltration and activation of V γ 9V δ 2T (TCR δ 2⁺ and Granzyme B⁺) and Car-B7H3- γ δ T cells (B7H3⁺ and Granzyme B⁺) peaked on

(See figure on next page.)

Fig. 3 The strategy for enhancing V γ 9V δ 2 T cell therapy in the treatment of glioma in the WAT group. V γ 9V δ 2 T cells were incubated with WAT primary glioma cells (TT-LS-luc, TT-YZJ-luc, TT-ZLH-luc, TT-XJ-luc, TT-SX-luc, and TT-HCL-luc) at E:T ratios of 1:1 in the presence or absence of ZOL (5 μ M) or BTN3A1 agonistic antibody (BTN3A1 20.1, 1 μ g/mL) for 18–20 h. The killing of V γ 9V δ 2 T cells against WAT primary glioma cells was significantly enhanced after ZOL stimulation **A** or BTN3A1 agonistic antibody stimulation **B**. Data are expressed as mean \pm SD. * $P < 0.05$, ** $P < 0.01$, *** $P < 0.001$, **** $P < 0.0001$. Car-B7H3- γ δ T cells had stronger and wider anti-glioma ability than parental V γ 9V δ 2 T cells in vitro. **(C)** CAR construct is shown. **(D)** V γ 9V δ 2 T cells and Car-B7H3- γ δ T cells were co-cultured with U87-B7H3-KO cells in a 1:1 ratio for 18–20 h in the presence or absence of ZOL (5 μ M). Luciferase activity was measured. Data are expressed as the mean \pm SD. **E** Flow cytometry analysis was performed to determine B7-H3 expression in WAT primary glioma cells. The expression of B7-H3 protein was higher than 90%. **F** V γ 9V δ 2 T cells and Car-B7H3- γ δ T cells were incubated with WAT primary glioma cells at E:T ratios of 1:1 for 18–20 h. Luciferase activity was measured. Data are expressed as the mean \pm SD. * $P < 0.05$, ** $P < 0.01$, *** $P < 0.001$. **G, H** The culture medium was collected, and ELISA was performed to measure IFN- γ and TNF- α levels. Data are expressed as the mean \pm SD. * $P < 0.05$, *** $P < 0.001$, **** $P < 0.0001$; n = 3

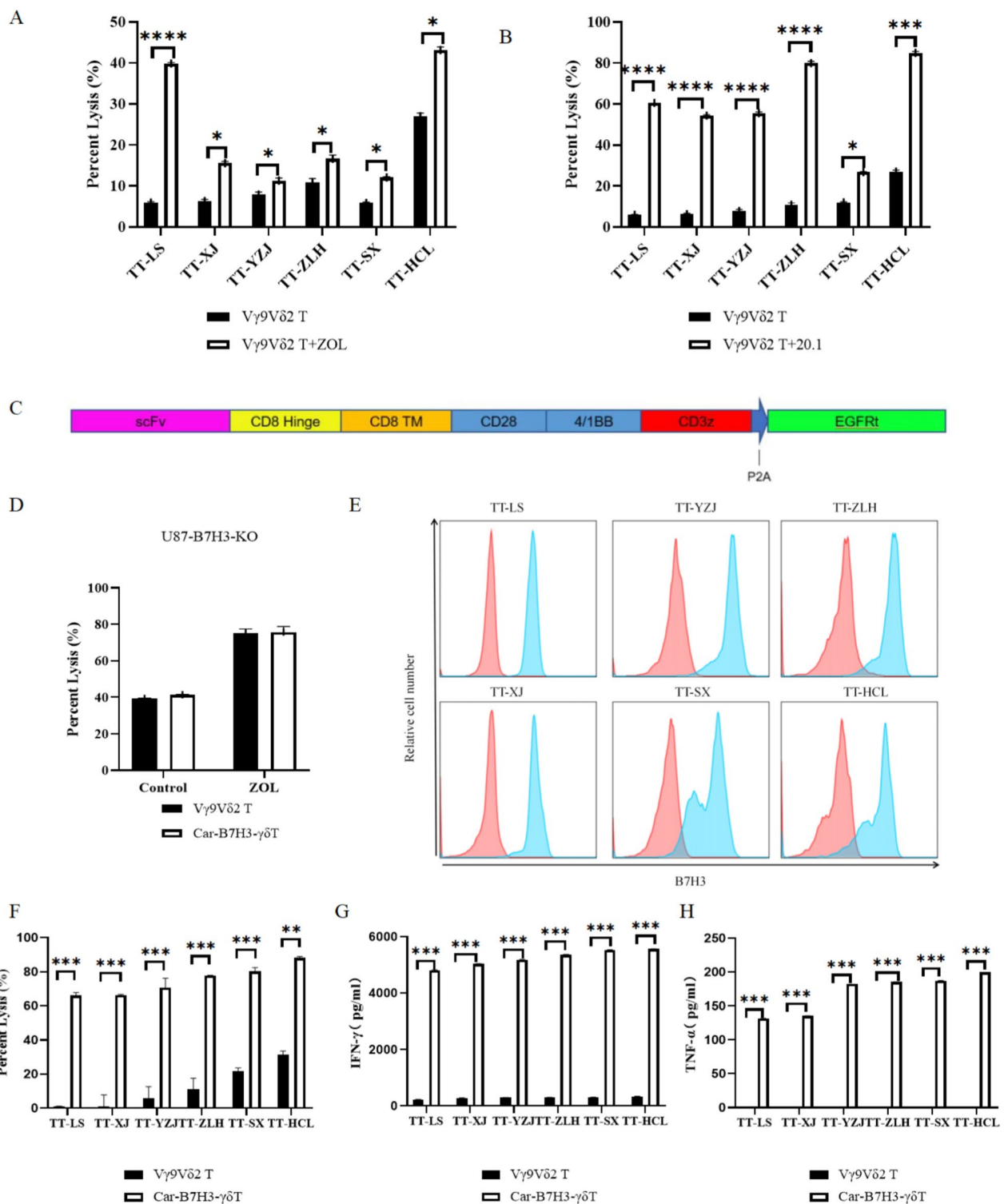


Fig. 3 (See legend on previous page.)

day 7, with more activated Car-B7H3- γ δ T cells infiltrating the tumor tissue. The infiltrations of both cell types decreased by day 14 (Fig. 5C), indicating that patients

could receive reinfusion therapy with V γ 9V δ 2T and Car-B7H3- γ δ T cells every two weeks in a clinical setting.

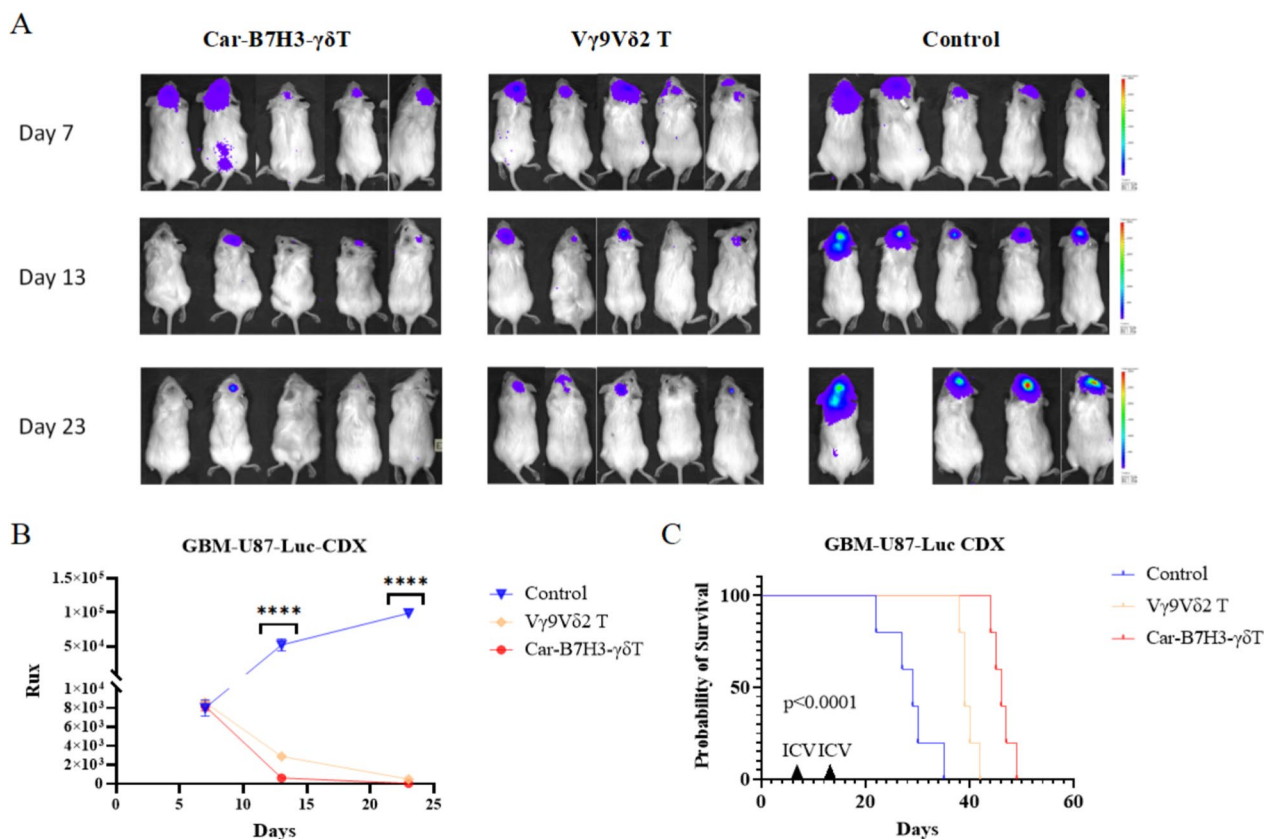


Fig. 4 The anti-glioma ability of Car-B7H3- $\gamma\delta$ T cells was stronger than that of parental V γ 9V δ 2 T cells in vivo **A** NSG mouse GBM models were treated with V γ 9V δ 2 T cells, Car-B7H3- $\gamma\delta$ T cells, or PBS ($n=5$). Bioluminescence images of the mouse brain were taken on day 7, 13, and 23 after injection. **B** Bioluminescence intensity was measured to examine tumor growth. Data are expressed as mean \pm SD. **** $P < 0.0001$. **C** Kaplan-Meier survival analysis was performed

V γ 9V δ 2 T and Car-B7H3- $\gamma\delta$ T therapy is safe against GBM tumors in mice after intracranial injection

We evaluated the safety of V γ 9V δ 2 T cell therapy by injecting low-dose (5×10^5 cells/5 μ L PBS) or high-dose (5×10^6 cells/5 μ L PBS) V γ 9V δ 2 T cells into the lateral ventricle of healthy NSG mice. H&E staining at 7 days after injection showed that V γ 9V δ 2 T cell therapy did not induce any significant histological changes in the liver, lung, ovary, brain, spleen, kidney, stomach, heart, or uterus of the mice compared to control treatment (Additional file 1: Figure S3A, S3B). Additionally, no significant change was observed in the body weight of the mice within 18 days after low or high dose of V γ 9V δ 2 T cell or Car-B7H3- $\gamma\delta$ T cell injection (Additional file 1: Figure S4A and S4B). These data suggest that V γ 9V δ 2 T cell therapy is well tolerated in NSG mice. To address the potential for cytokine release syndrome and neurotoxicity from immune cells [34], we measured the serum inflammatory cytokine levels of the mice and found no significant differences among the three groups ($P > 0.05$) (Additional file 1: Figure S4C).

Discussion

While the current standard therapies for glioma, including surgery, radiotherapy, and chemotherapy, have been employed, the prognosis for patients remains suboptimal. V γ 9V δ 2 T cell immunotherapy offers a promising approach. In this study, we demonstrated that V γ 9V δ 2 T cells derived from healthy human PBMCs inhibited GBM cell proliferation in vitro and suppressed GBM tumor growth in vivo without apparent toxicity to mice, consistent with recent reports [35–37]. However, the response to V γ 9V δ 2 T cell therapy varied greatly among PTCs, leading us to classify them into SAT and WAT groups. We therefore aimed to identify potential indicators associated with the response to V γ 9V δ 2 T cell therapy. IHC staining conducted on matched tumor tissue samples from PTCs in the SAT group confirmed the elevated expression levels of BTN2A1 and BTN3A1. Intriguingly, V γ 9V δ 2 T cells elicited a strong antitumor effect in 23.1% of PTCs, which was significantly associated with higher expression levels of BTN2A1 and BTN3A1. These findings suggest that BTN2A1 and BTN3A1 hold promise

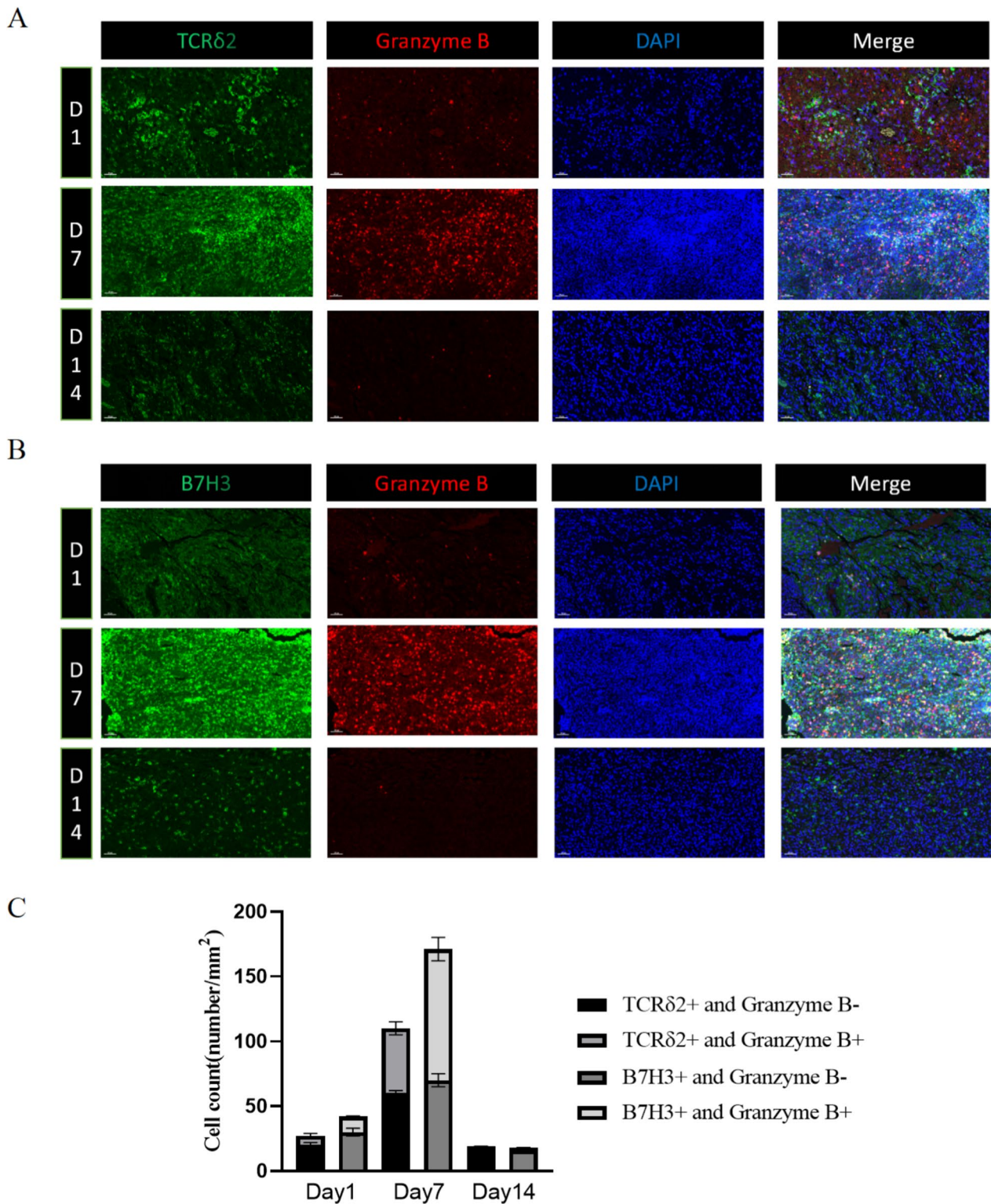


Fig. 5 Vγ9Vδ2 T cells and Car-B7H3-γδT cells infiltrated into tumor xenografts in mice Tumor-bearing mice received an intracranial injection of 5×10^6 Vγ9Vδ2 T cells **A** or Car-B7H3-γδT cells **B**, followed by multiplex immunofluorescence staining to detect human TCRδ2, B7H3, and Granzyme B expression in tumor xenografts on day 1, day 7, and day 14 after injection. **C** The percentage of activated Vγ9Vδ2T (TCRδ2⁺ and Granzyme B⁺) cells and Car-B7H3-γδT (B7H3⁺ and Granzyme B⁺) cells (number /mm²) in total Vγ9Vδ2 T cells at different time points was analyzed. Data are expressed as the mean ± SD

as potential indicators for the response of GBM patients to V γ 9V δ 2 T cell therapy. To translate this finding from bench to bedside, further data from a larger cohort is required. In addition, a more convenient method to detect BTN2A1 and BTN3A1 expression would be necessary. Dysregulation of the mevalonate pathway is common in tumor cells, leading to the accumulation of both DMAPP and IPP, which could be recognized by V γ 9V δ 2 T cells [38–40]. Our RNA-seq analysis of SAT and WAT tissues further revealed the involvement of lipid metabolism and inflammation-related pathways in the antitumor effect of V γ 9V δ 2 T cells, providing valuable insights for future studies.

Although V γ 9V δ 2 T cells derived from human PBMCs demonstrated good cytotoxicity against gliomas that overexpress BTN2A1/BTN3A1, such overexpression occurred in less than 30% of GBM cases. This led us to explore the use of zoledronate, a bisphosphonate drug that inhibits farnesyl diphosphate synthase to accumulate DMAPP and IPP, or a BTN3A1 agonistic antibody 20.1 to sensitize WAT primary glioma cells to V γ 9V δ 2 T cell killing. Recognizing the clinical limitations of ZOL and BTN3A1 agonistic antibody in glioma, especially given the high B7H3 expression in the majority of GBM cases, we genetically engineered V γ 9V δ 2 T cells into Car-B7H3- γ δ T cells. Importantly, Car-B7H3- γ δ T cells can recognize tumors via B7H3-Car and also possess the ability to eliminate tumors through phosphoantigen recognition. Our study showed that Car-B7H3- γ δ T cells were more potent than unmodified V γ 9V δ 2 T cells at inhibiting GBM cell proliferation in vitro and improving the overall survival of tumor-bearing mice, suggesting that genetic modification of V γ 9V δ 2 T cells may enhance the therapeutic efficacy and clinical outcomes of V γ 9V δ 2 T cell-based immunotherapy for GBM. Although V γ 9V δ 2 T cells derived from human PBMCs demonstrated good cytotoxicity against gliomas that overexpress BTN2A1/BTN3A1, such overexpression occurred in less than 30% of GBM cases. Therefore, Car-B7H3- γ δ T cells show greater promise as a potential therapeutic agent for GBM treatment compared to unmodified V γ 9V δ 2 T cells.

As γ δ T cell numbers and exercise responsiveness decline with age [44], PBMCs from healthy donors aged 18–24 years were used in this study. However, the specific immune status, the blood–brain barrier, and the lack of a classical lymphatic drainage system in the central nervous system (CNS) can hinder the delivery of effector T cells [45]. Clinical trials of adoptive immunotherapy with human T lymphocytes for GBM have employed intravascular, intratumoral, or intraventricular injection [46]. However, intravascular administration may cause

cytokine release syndrome and tumor inflammation-associated neurotoxicity, while intratumoral injection may cause tumor hemorrhage or increased cranial pressure [47]. To prevent intracranial hypertension, a small amount of cerebrospinal fluid can be extracted before intracerebroventricular injection. Therefore, we chose to perform the in vivo study using intracerebroventricular injection. Consistent with studies using this injection method [48–50], our study showed that intracerebroventricular injection of V γ 9V δ 2 T cells and Car-B7H3- γ δ T cells effectively inhibited brain tumor growth in the absence of small molecule phosphate drugs. Moreover, V γ 9V δ 2 T cells and Car-B7H3- γ δ T cells were well tolerated in mice and could infiltrate into the tumor tissue. Although TCR δ 2 expression was barely detectable in tumor tissue at 14 days after treatment, V γ 9V δ 2 T cells and Car-B7H3- γ δ T cells displayed potent tumor inhibitory effects within 14 days after injection. These data suggest that intracerebroventricular injection of V γ 9V δ 2 T cells and Car-B7H3- γ δ T cells is clinically feasible for GBM treatment.

In conclusion, the high expression of BTN2A1/BTN3A1 may serve as a potential indicator for pre-screening V γ 9V δ 2 T cells derived from healthy human PBMCs for glioma treatment. The potent antitumor effect of V γ 9V δ 2 T cells on PTCs may be related to lipid metabolism and inflammation-related pathways. Car-B7H3- γ δ T cells exhibit stronger anti-glioma abilities compared to parental V γ 9V δ 2 T cells in vitro and demonstrated improved prognostic outcomes in tumor-bearing mice. These findings suggest that γ δ T cells represent a promising therapeutic agent for GBM.

Abbreviations

GBM	Glioblastoma
WHO	World Health Organization
TCR	T cell receptor
BTN2A1	Butyrophilin subfamily 2 member A1
MICA/B	MHC class I-related chain proteins A and B
CAR	Chimeric antigen receptor
PBMCs	Peripheral blood mononuclear cells
PTCs	Patient-derived tumor cell clusters
EGFRt	Epidermal growth factor receptor
RNA-Seq	RNA sequencing
SAT	Stronger antitumor effect
WAT	Weaker antitumor effect
PBS	Phosphate-buffered saline
IHC	Immunohistochemistry
MIS	Multiplex immunofluorescence staining
DEGs	Differentially expressed genes
GSEA	Gene set enrichment analysis
PBMCs	Peripheral blood mononuclear cells
SD	Standard deviation
H&E	Hematoxylin & eosin
ICV	Lateral cerebral ventricle
ZOL	Zoledronic acid

Supplementary Information

The online version contains supplementary material available at <https://doi.org/10.1186/s12967-023-04514-8>.

Additional file 1: Figure S1. Hematoxylin and eosin staining of xenograft tumor sample from NSG mouse. Magnification 20 ×. Scale bar = 50 μm. **Figure S2.** A Flow cytometry analysis was conducted to detect the expression of BTN2A1 and BTN3A1 in GBM cell lines. B Car-B7H3-γδT cells were obtained by transfecting Vγ9Vδ2 T cells with plasmids containing scFv of the anti-B7-H3 antibody. Flow cytometry analysis was used to determine the purity of Car-B7H3-γδT cells. C Flow cytometry analysis was performed to determine B7-H3 expression in U87-MG, TJ905, and HTB15 cells. The protein expression of B7-H3 was 92.6%, 91.8%, and 93.2% in U-87MG, TJ905, and HTB15, respectively. D Vγ9Vδ2 T or Car-B7H3-γδT cells were incubated with U-87MG-Luc, TJ905-Luc, or HTB15-Luc cells at different effective target (E:T) ratios of 0:1, 0.5:1, 1:1, or 3:1 in the presence of IL-2. The luciferase activity was measured to determine the cell viability of GBM cells at 18–20 h. E The culture medium was collected. ELISA was performed to measure IFN-γ and TNF-α levels. Data are expressed as the mean ± SD. **P* < 0.05, ****P* < 0.001, *****P* < 0.0001; *n* = 3. **Figure S3.** Hematoxylin and eosin staining of the liver, lung, ovary, brain, spleen, kidney, stomach, heart, and uterus tissue samples from NSG mice after injection with PBS A or high-dose (5 × 10⁶ cells/5 μL PBS) Vγ9Vδ2 T cells B. Magnification 10 ×. **Figure S4.** Evaluation of Vγ9Vδ2 T and Car-B7H3-γδT cell toxicity. A The body weights of mice were measured at different time points after intraventricular injection of control (PBS), low-dose of Vγ9Vδ2 T cells (5 × 10⁵ cells/5 μL PBS), or high-dose of Vγ9Vδ2 T cells (5 × 10⁶ cells/5 μL PBS). B The body weights of GBM tumor-bearing mice were measured at different time points after intraventricular injection. C Cytokine multiplex assay was carried out to examine mouse serum cytokine alterations at 7 days after T cell therapy. Z-score of each cytokine was calculated as the mean fluorescence intensity. A heatmap of the z-scores ranging from −3 to 3 was generated. **Table S1.** Basic characteristics of all PTC patients. **Table S2. A** Primary antibody used in Multiplex staining. **B** Experimental conditions and procedures of Multiplex staining of TCRδ2 panel. **C.** Experimental conditions and procedures of Multiplex staining of B7H3 panel. **Table S3.** Relationship between different grades of glioma and different responses to Vγ9Vδ2 T therapy.

Acknowledgements

We thank Xuefeng Guo for the assistance during the initial phase of this study.

Author contributions

TS, YHZ, and WLZ designed the experiments. YW and WWM performed the experiments, analyzed the data, and generated the figures. YW wrote the manuscript, and TS, NJ, YZ, CCP, PZ, XGZ and MZC contributed to its preparation. TS, JJX, YHZ, and LWZ supervised all project activities.

Funding

This work was supported by Beijing Municipal Natural Science Foundation (Z190015) and public welfare development and reform pilot project of Beijing municipal medical research institutes (Beijing medical research 2018–7).

Availability of data and materials

All data generated or analysed during this study are included in this published article [and its Additional file information files].

Declarations

Ethics approval and consent to participate

The study was approved by the Ethics Committee of Beijing Tiantan Hospital (KY2014-021–02) and conducted according to the guidelines of the Declaration of Helsinki. All participants provided signed informed consent. All animal procedures were conducted following the guidelines of the Beijing Neurosurgical Institute Laboratory Animal Welfare and Ethics Committee (BNI approval number: 202202002) and in accordance with the AAALAC and IACUC Guidelines.

Consent for publication

Not applicable.

Competing interests

The authors declare that they have no competing interests.

Author details

¹Beijing Advanced Innovation Center for Biomedical Engineering, Beijing Advanced Innovation Center for Big Data-Based Precision Medicine, Beihang University, Beijing 100191, China. ²Department of Neurosurgery, Beijing Tiantan Hospital, Capital Medical University, Beijing 100070, China. ³China National Clinical Research Center for Neurological Diseases, Beijing 100070, China. ⁴Tsinghua-Peking Center for Life Sciences, State Key Laboratory of Membrane Biology, School of Pharmaceutical Sciences, Tsinghua University, Beijing 100084, China. ⁵Jiangsu Institute of Clinical Immunology, First Affiliated Hospital, Jiangsu Provincial Key Laboratory of Stem Cell and Biomedical Materials, Soochow University, Soochow University, Suzhou 215000, China. ⁶State Key Laboratory of Natural and Biomimetic Drugs, Institute of Molecular Medicine, Department of Biomedical Engineering, College of Engineering, Peking University, Beijing 100871, China.

Received: 6 July 2023 Accepted: 7 September 2023

Published online: 28 September 2023

References

- Louis DN, Perry A, Reifenberger G, von Deimling A, Figarella-Branger D, Cavenee WK, Ohgaki H, Wiestler OD, Kleihues P, Ellison DW. The 2016 World Health Organization classification of tumors of the central nervous system: a summary. *Acta Neuropathol.* 2016;131:803–20.
- Ostrom QT, Patil N, Cioffi G, Waite K, Kruchko C, Barnholtz-Sloan JS. CBTRUS statistical report: primary brain and other central nervous system tumors diagnosed in the United States in 2013–2017. *Neuro Oncol.* 2020;22:96.
- Stupp R, Mason WP, van den Bent MJ, Weller M, Fisher B, Taphoorn MJ, Belanger K, Brandes AA, Marosi C, Bogdahn U, et al. Radiotherapy plus concomitant and adjuvant temozolomide for glioblastoma. *N Engl J Med.* 2005;352:987–96.
- Gittleman H, Boscia A, Ostrom QT, Truitt G, Fritz Y, Kruchko C, Barnholtz-Sloan JS. Survivorship in adults with malignant brain and other central nervous system tumor from 2000–2014. *Neuro Oncol.* 2018;20:vii16.
- Mitchell DA, Cui X, Schmittling RJ, Sanchez-Perez L, Snyder DJ, Congdon KL, Archer GE, Desjardins A, Friedman AH, Friedman HS, et al. Monoclonal antibody blockade of IL-2 receptor alpha during lymphopenia selectively depletes regulatory T cells in mice and humans. *Blood.* 2011;118:3003–12.
- Wang QT, Nie Y, Sun SN, Lin T, Han RJ, Jiang J, Li Z, Li JQ, Xiao YP, Fan YY, et al. Tumor-associated antigen-based personalized dendritic cell vaccine in solid tumor patients. *Cancer Immunol Immunother.* 2020;69:1375–87.
- Weenink B, French PJ, Sillevius Smitt PAE, Debets R, Geurts M. Immunotherapy in glioblastoma: current shortcomings and future perspectives. *Cancers.* 2020;12(3):751.
- Bryant NL, Suarez-Cuervo C, Gillespie GY, Markert JM, Nabors LB, Meleth S, Lopez RD, Lamb LS Jr. Characterization and immunotherapeutic potential of gammadelta T-cells in patients with glioblastoma. *Neuro Oncol.* 2009;11:357–67.
- Lamb LS Jr. Gammadelta T cells as immune effectors against high-grade gliomas. *Immunol Res.* 2009;45:85–95.
- Silva-Santos B, Serre K, Norell H. gammadelta T cells in cancer. *Nat Rev Immunol.* 2015;15:683–91.
- Riganti C, Massaia M, Davey MS, Eberl M. Human gammadelta T-cell responses in infection and immunotherapy: common mechanisms, common mediators? *Eur J Immunol.* 2012;42:1668–76.
- Rigau M, Ostrouska S, Fulford TS, Johnson DN, Woods K, Ruan Z, McWilliam HEG, Hudson C, Tutuka C, Wheatley AK, et al. Butyrophilin-2A1 is essential for phosphoantigen reactivity by gammadelta T cells. *Science.* 2020;367:5516.
- Karunakaran MM, Willcox CR, Salim M, Paletta D, Fichtner AS, Noll A, Starick L, Nohren A, Begley CR, Berwick KA, et al. Butyrophilin-2A1 directly binds germline-encoded regions of the Vgamma9Vdelta2 TCR and is essential for phosphoantigen sensing. *Immunity.* 2020;52(487–498): e486.

14. Starick L, Riano F, Karunakaran MM, Kunzmann V, Li J, Kreiss M, Amslinger S, Scotet E, Olive D, De Libero G, Herrmann T. Butyrophilin 3A (BTN3A, CD277)-specific antibody 20.1 differentially activates Vgamma9Vdelta2 TCR clonotypes and interferes with phosphoantigen activation. *Eur J Immunol*. 2017;47:982–92.
15. Correia DV, Lopes A, Silva-Santos B. Tumor cell recognition by gamma-delta T lymphocytes: T-cell receptor vs NK-cell Receptors. *Oncimmunol*. 2013;2: e22892.
16. Chitadze G, Lettau M, Luecke S, Wang T, Janssen O, Furst D, Mytilineos J, Wesch D, Oberg HH, Held-Feindt J, Kabelitz D. NKG2D- and T-cell receptor-dependent lysis of malignant glioma cell lines by human gamma-delta T cells: modulation by temozolomide and A disintegrin and metalloproteases 10 and 17 inhibitors. *Oncimmunology*. 2016;5: e1093276.
17. Friese MA, Platten M, Lutz SZ, Naumann U, Aulwurm S, Bischof F, Buhring HJ, Dichgans J, Rammensee HG, Steinle A, Weller M. MICA/NKG2D-mediated immunogene therapy of experimental gliomas. *Cancer Res*. 2003;63:8996–9006.
18. Hsiao CH, Lin X, Barney RJ, Shippy RR, Li J, Vinogradova O, Wiemer DF, Wiemer AJ. Synthesis of a phosphoantigen prodrug that potentially activates Vgamma9Vdelta2 T-lymphocytes. *Chem Biol*. 2014;21:945–54.
19. Safarzadeh Kozani P, Safarzadeh Kozani P, Rahbarizadeh F. Addressing the obstacles of CAR T cell migration in solid tumors: wishing a heavy traffic. *Crit Rev Biotechnol*. 2021;4:1–20.
20. Dana H, Chalbatani GM, Jalali SA, Mirzaei HR, Grupp SA, Suarez ER, Raposo C, Webster TJ. CAR-T cells: Early successes in blood cancer and challenges in solid tumors. *Acta Pharm Sin B*. 2021;11:1129–47.
21. Rozenbaum M, Meir A, Aharony Y, Itzhaki O, Schachter J, Bank I, Jacoby E, Besser MJ. Gamma-delta CAR-T cells show CAR-directed and independent activity against leukemia. *Front Immunol*. 2020;11:1347.
22. Qin VM, D'Souza C, Neeson PJ, Zhu JJ. Chimeric antigen receptor beyond CAR-T Cells. *Cancers*. 2021;13:404.
23. Nehama D, Di Ianni N, Musio S, Du H, Patane M, Pollo B, Finocchiaro G, Park JH, Dunn DE, Edwards DS, et al. B7-H3-redirected chimeric antigen receptor T cells target glioblastoma and neurospheres. *EBioMedicine*. 2019;47:33–43.
24. Du H, Hirabayashi K, Ahn S, Kren NP, Montgomery SA, Wang X, Tiruthani K, Mirlekar B, Michaud D, Greene K, et al. antitumor responses in the absence of toxicity in solid tumors by targeting B7–H3 via chimeric antigen receptor T cells. *Cancer Cell*. 2019;35(221–237): e228.
25. Majzner RG, Theruvath JL, Nellan A, Heitzeneder S, Cui Y, Mount CW, Rietberg SP, Linde MH, Xu P, Rota C, et al. CAR T cells targeting B7–H3, a pan-cancer antigen, demonstrate potent preclinical activity against pediatric solid tumors and brain tumors. *Clin Cancer Res*. 2019;25:2560–74.
26. Kramer K, Kushner BH, Modak S, Pandit-Taskar N, Smith-Jones P, Zanzonico P, Humm JL, Xu H, Wolden SL, Souweidane MM, et al. Compartmental intrathecal radioimmunotherapy: results for treatment for metastatic CNS neuroblastoma. *J Neurooncol*. 2010;97:409–18.
27. Xu Y, Xiang Z, Alnaggar M, Kouakanou L, Li J, He J, Yang J, Hu Y, Chen Y, Lin L, et al. Allogeneic Vgamma9Vdelta2 T-cell immunotherapy exhibits promising clinical safety and prolongs the survival of patients with late-stage lung or liver cancer. *Cell Mol Immunol*. 2021;18:427–39.
28. Guedan S, Posey AD Jr, Shaw C, Wing A, Da T, Patel PR, McGettigan SE, Casado-Medrano V, Kawalekar OU, Uribe-Herranz M, et al. Enhancing CAR T cell persistence through ICOS and 4–1BB costimulation. *JCI Insight*. 2018;3:1.
29. Roselli E, Boucher JC, Li G, Kotani H, Spitzer K, Reid K, Cervantes EV, Bulliard Y, Tu N, Lee SB, et al. 4–1BB and optimized CD28 co-stimulation enhances function of human mono-specific and bi-specific third-generation CAR T cells. *J Immunother Cancer*. 2021;9:3354.
30. Yin S, Xi R, Wu A, Wang S, Li Y, Wang C, Tang L, Xia Y, Yang D, Li J, et al. Patient-derived tumor-like cell clusters for drug testing in cancer therapy. *Sci Transl Med*. 2020. <https://doi.org/10.1126/scitranslmed.aaz1723>.
31. Cano CE, Pasero C, De Gassart A, Kerneur C, Gabriac M, Fullana M, Granarolo E, Hoet R, Scotet E, Rafia C, et al. BTN2A1, an immune checkpoint targeting Vgamma9Vdelta2 T cell cytotoxicity against malignant cells. *Cell Rep*. 2021;36: 109359.
32. Vavassori S, Kumar A, Wan GS, Ramanjaneyulu GS, Cavallari M, El Daker S, Beddoe T, Theodossis A, Williams NK, Gostick E, et al. Butyrophilin 3A1 binds phosphorylated antigens and stimulates human gamma-delta T cells. *Nat Immunol*. 2013;14:908–16.
33. Okuno D, Sugiura Y, Sakamoto N, Tagod MSO, Iwasaki M, Noda S, Tamura A, Senju H, Umeiyama Y, Yamaguchi H, et al. Comparison of a novel bisphosphonate prodrug and zoledronic acid in the induction of cytotoxicity in human Vgamma2Vdelta2 T cells. *Front Immunol*. 2020;11:1405.
34. Theruvath J, Sotillo E, Mount CW, Graef CM, Delaidelli A, Heitzeneder S, Labanieh L, Dhingra S, Leruste A, Majzner RG, et al. Locoregionally administered B7-H3-targeted CAR T cells for treatment of atypical teratoid/rhabdoid tumors. *Nat Med*. 2020;26:712–9.
35. Choi H, Lee Y, Park SA, Lee JH, Park J, Park JH, Lee HK, Kim TG, Jeun SS, Ahn S. Human allogeneic gamma-delta T cells kill patient-derived glioblastoma cells expressing high levels of DNAM-1 ligands. *Oncimmunology*. 2022;11:2138152.
36. Lee M, Park C, Woo J, Kim J, Kho I, Nam DH, Park WY, Kim YS, Kong DS, Lee HW, Kim TJ. Preferential infiltration of unique Vgamma9Jgamma2-Vdelta2 T cells into glioblastoma multiforme. *Front Immunol*. 2019;10:555.
37. Rosso DA, Rosato N, Iturrizaga J, Shiromizu CM, Keitelman IA, Coronel JV, Gomez FD, Amaral MM, Rabadan AT, et al. Glioblastoma cells potentiate the induction of the Th1-like profile in phosphoantigen-stimulated gamma-delta T lymphocytes. *J Neurooncol*. 2021;153:403–15.
38. Zhou X, Gu Y, Xiao H, Kang N, Xie Y, Zhang G, Shi Y, Hu X, Oldfield E, Zhang X, Zhang Y. Combining Vgamma9Vdelta2 T Cells with a Lipophilic Bisphosphonate Efficiently Kills Activated Hepatic Stellate Cells. *Front Immunol*. 2017;8:1381.
39. Yang Y, Li L, Yuan L, Zhou X, Duan J, Xiao H, Cai N, Han S, Ma X, Liu W, et al. A Structural change in butyrophilin upon phosphoantigen binding underlies phosphoantigen-mediated Vgamma9Vdelta2 T cell activation. *Immunity*. 2019;50(1043–1053): e1045.
40. Xia Y, Xie Y, Yu Z, Xiao H, Jiang G, Zhou X, Yang Y, Li X, Zhao M, Li L, et al. The mevalonate pathway is a druggable target for vaccine adjuvant discovery. *Cell*. 2018;175(1059–1073): e1021.
41. Maggs L, Cattaneo G, Dal AE, Moghaddam AS, Ferrone S. CAR T Cell-based immunotherapy for the treatment of glioblastoma. *Front Neurosci*. 2021;15: 662064.
42. Lin YJ, Mashouf LA, Lim M. CART cell therapy in primary brain tumors: current investigations and the future. *Front Immunol*. 2022;13: 817296.
43. Digregorio M, Coppieters N, Lombard A, Lumapat PN, Scholtes F, Rogister B. The expression of B7–H3 isoforms in newly diagnosed glioblastoma and recurrence and their functional role. *Acta Neuropathol Commun*. 2021;9:59.
44. Pistillo M, Bigley AB, Spielmann G, LaVoy EC, Morrison MR, Kunz H, Simpson RJ. The effects of age and viral serology on gamma-delta T-cell numbers and exercise responsiveness in humans. *Cell Immunol*. 2013;284:91–7.
45. Bailey SL, Carpentier PA, McMahon EJ, Begolka WS, Miller SD. Innate and adaptive immune responses of the central nervous system. *Crit Rev Immunol*. 2006;26:149–88.
46. Sloan AE, Dansey R, Zamorano L, Barger G, Hamm C, Diaz F, Baynes R, Wood G. Adoptive immunotherapy in patients with recurrent malignant glioma: preliminary results of using autologous whole-tumor vaccine plus granulocyte-macrophage colony-stimulating factor and adoptive transfer of anti-CD3-activated lymphocytes. *Neurosurg Focus*. 2000;9: e9.
47. Majzner RG, Ramakrishna S, Yeom KW, Patel S, Chinnasamy H, Schultz LM, Richards RM, Jiang L, Barsan V, Mancusi R, et al. GD2-CAR T cell therapy for H3K27M-mutated diffuse midline gliomas. *Nature*. 2022. <https://doi.org/10.1038/s41586-022-04489-4>.
48. Jarry U, Joalland N, Chauvin C, Clemenceau B, Pecqueur C, Scotet E. Stereotactic adoptive transfer of cytotoxic immune cells in murine models of orthotopic human glioblastoma multiforme xenografts. *J Vis Exp*. 2018. <https://doi.org/10.3791/57870>.
49. Joalland N, Chauvin C, Oliver L, Vallette FM, Pecqueur C, Jarry U, Scotet E. IL-21 increases the reactivity of allogeneic human vgamma-9Vdelta2 T cells against primary glioblastoma tumors. *J Immunother*. 2018;41:224–31.
50. Chauvin C, Joalland N, Perroteau J, Jarry U, Lafrance L, Willem C, Retiere C, Oliver L, Gratas C, Gautreau-Rolland L, et al. NKG2D controls natural reactivity of Vgamma9Vdelta2 T lymphocytes against mesenchymal glioblastoma cells. *Clin Cancer Res*. 2019;25:7218–28.
51. Madhok A, Bhat SA, Philip CS, Sureshbabu SK, Chiplunkar S, Galande S. Transcriptome signature of Vgamma9Vdelta2 T cells treated with phosphoantigens and notch inhibitor reveals interplay between TCR and notch signaling pathways. *Front Immunol*. 2021;12: 660361.

52. Miyashita M, Shimizu T, Ashihara E, Ukimura O. Strategies to improve the antitumor effect of gammadelta T cell immunotherapy for clinical application. *Int J Mol Sci*. 2021. <https://doi.org/10.3390/ijms22168910>.
53. Huang C, Xiang Z, Zhang Y, Li Y, Xu J, Zhang H, Zeng Y, Tu W. NKG2D as a cell surface marker on gammadelta-T cells for predicting pregnancy outcomes in patients with unexplained repeated implantation failure. *Front Immunol*. 2021;12: 631077.
54. Xiang Z, Tu W. Dual face of Vgamma9Vdelta2-T cells in tumor immunology: anti—versus pro-tumoral activities. *Front Immunol*. 2017;8:1041.
55. Yang R, Zhao Y, Gu Y, Yang Y, Gao X, Yuan Y, Xiao L, Zhang J, Sun C, Yang H, et al. Isocitrate dehydrogenase 1 mutation enhances 24(S)-hydroxycholesterol production and alters cholesterol homeostasis in glioma. *Oncogene*. 2020;39:6340–53.

Publisher's Note

Springer Nature remains neutral with regard to jurisdictional claims in published maps and institutional affiliations.

Ready to submit your research? Choose BMC and benefit from:

- fast, convenient online submission
- thorough peer review by experienced researchers in your field
- rapid publication on acceptance
- support for research data, including large and complex data types
- gold Open Access which fosters wider collaboration and increased citations
- maximum visibility for your research: over 100M website views per year

At BMC, research is always in progress.

Learn more biomedcentral.com/submissions

